



Research paper

Study on mechanical properties of notched steel wire under tension and bending

Hongyu Fei¹, Quansheng Sun², Jianxi Yang³

Abstract: The fracture reason of steel wire cable is complex, and the corrosion and local bending effect of anchorage end of steel wire cable under tension are one of the main factors. Taking the steel wire of an arch bridge cable as the research object, the notch method was used to simulate the corrosion pits on the surface of the steel wire, and the tension and bending mechanical properties of the high strength notched steel wire were tested. The bending finite element model of the high strength steel wire was established by ANSYS WORKBENCH, and the tension and bending mechanical properties of the notched steel wire under different vertical loads and pretension were studied. The test and calculation results show that the test data are close to the finite element calculation results and the variation law is consistent. Under the same vertical load, the deformation of steel wire notch decreases with the increase of pretension; The stress at the bottom of the notch is the largest at 180° direction and the smallest at 90° direction of the vertical load. Under the same vertical load and pretension, the stress of spherical shape at the notch is the largest, followed by ellipsoid shape, and groove shape is the smallest, and there is a high stress zone at the edge of groove shape. When the pretension is applied, the initial stress increases with the increase of pretension, while the stress at the notch caused by bending decreases with the increase of pretension.

Keywords: artificial notch, finite element analysis, high strength steel wire, mechanical properties, tension and bending effect

¹MSc., School of Civil Engineering, Northeast Forestry University, 150040 Harbin, China, e-mail: fei-hongyu357@126.com, ORCID: 0000-0002-3450-0834

²Prof., PhD., Eng., School of Civil Engineering, Northeast Forestry University, 150040 Harbin, China, e-mail: sunquansheng@nefu.edu.cn, ORCID: 0000-0002-7772-3499

³PhD., School of Civil Engineering, Northeast Forestry University, 150040 Harbin, China, e-mail: yangjianxi@nefu.edu.cn, ORCID: 0000-0002-9860-3410

1. Introduction

The suspender is an important component of the suspender arch bridge, which transmits the load of the bridge deck system to the arch rib and is the link to transmit the load. In recent years, arch bridge collapse accidents caused by suspender fracture are common, such as Nanfang Macao-crossing Bridge in Yilan, Taiwan Province, China (2019) and South Central Ring Bridge in Taiyuan, Shanxi Province, China (2022). These accidents have caused varying degrees of casualties. During the long service of the arch bridge, the inner steel wire will be corroded in different degrees due to the damage of derrick sheath. However, under the action of vibration generated by temperature load and vehicle load, the anchorage end of the derrick will appear serious local bending phenomenon, resulting in uneven local force of the derrick and increasing effect [1, 2]. The suspender sheath and the outermost ring steel wire are in a high stress state for a long time. The sheath at the bending of the suspender anchorage end is easily damaged, resulting in corrosion of the steel wire at the break [3, 4]. Under the long-term tension and bending, the anchorage end of the suspender will produce mechanical fatigue, and the local corrosion of the steel wire will produce corrosion pits. Finally, under the coupling of corrosion and high stress, the suspender internal steel wire is fracture, until the suspender is completely broken.

At present, domestic and foreign scholars have made some research on the bending mechanical properties of steel wire cable, and have made some achievements. Many foreign scholars have studied the bending mechanical properties of spiral steel wire cable. Raof [5] and his research team used elastic bending thin rod theory to study the contact stress, bending hysteresis behavior and fatigue characteristics of simple helix steel strand, closed helix steel strand and helix steel strand with axial prestress. Papailiou [6] studied the bending mechanical behavior of steel wire cable by Euler-Bernoulli beam theory. It is concluded that the tensile force of steel wire under slip state can be determined by the mechanical equilibrium equation of steel wire under the action of maximum friction force, and the slip of steel wire begins near the neutral axis, and the bending stiffness of the cable changes smoothly from the bonding of steel wire to the slip state. Hong [7] developed the Papailiou's bending mechanical model, and established the mesoscale mechanical model of the bending behavior of the closed spiral steel wire cable under the action of tension. The model considered the nonlinear dissipation behavior of the steel wire sliding under the action of friction, and obtained that the bending stiffness decreased rapidly with the increase of the cable curvature, and obtained the approximate upper limit value of the bending curvature of the cable under the axial force and small bending. Khan [8] proposed a modified mechanical model of cable bending, mainly studied the bending mechanical behavior of helical wire cables, enclosed wire cables and sheathed wire cables used in deep water under the action of tension and bending, and gave a simplified method to determine the bending stiffness of multi-layer helical wire cables with large diameter. Foti [9, 10] proposed a fine mechanical model of cable bending using a homogeneous beam unit, studied shear lag bending mechanical behavior, and deduced the steel strand cable mechanics model under axial force and bending. By defining the wire sliding limit area (the permissible value range of axial force), Foti studied the sliding conditions of the interlayer steel wire and gave the closed-form solution of wire slip under uniform bending condition. Matuszkiewicz [11] proposed an analytical calculation method for the structure containing cable elements, which demonstrated that

the permanent deformation of the wire rope may occur when the wire rope is used without pre-tension, which will affect the shape of the wire rope and may significantly reduce the force value in the wire rope. Domestic scholars have done a lot of research on the bending mechanical properties of steel wire cables. Chen [12] carried out static bending tests of semi-parallel steel wire cables with free ends, weld ends and pretension at both ends. It is concluded that the load-displacement curve of free ends cable under bending is elastic-plastic. The welding end cable ensures the integrity of the cable but the strengthening effect is weak and limited. The bending stiffness of the pretensioned cable at both ends increases with the increase of the pretension level, but decreases with the increase of the cable size. Yu [13] simplified the extrusion and friction slip between steel wires into the spring action in three directions, and established a semi-fine finite element model of beam-beam spring combination to study the bending mechanical properties of steel wire cables. Zhang [14, 15] used the laminated beam theory to establish the theoretical mechanical model of parallel steel wire cable bending considering interlayer contact friction and studied the change rule of bending stiffness of steel wire cable. Through experimental verification, the theoretical model is consistent with the experimental data. In summary, the current research on tensile-bending mechanical properties of cables mainly focuses on intact cables and focuses on undamaged steel wire cables. However, for the actual arch bridge suspenders, they are often operated with damage, and the local bending of the upper and lower anchorage ends is serious. Especially, the lower anchorage end contacting with the bridge deck is often the key area of sheath damage, and the steel wire corrosion is also serious. The finite element numerical study also shows that under the action of pretension, corrosion pits will lead to uneven distribution of local stress of high-strength steel wire [16], so it is necessary to study the mechanical properties of steel wire cables considering corrosion under tension and bending.

In this paper, the high-strength steel wire in the suspender is taken as the research object, and the local corrosion pits of steel wire are simulated by artificial notch. The counterforce frame is designed and made to carry out the tensile-bending coupling mechanical properties test of the high-strength steel wire with artificial notch. At the same time, using the finite element software ANSYS WORKBENCH, the finite element numerical model of steel wire bending is established and verified by experimental data. Finally, the effects of different pretensions, notch shapes, bending loads and loading directions on the stress and stiffness of the high-strength steel wire with notch are analyzed, which provides the basis for the subsequent research on the bending mechanical properties and bearing capacity evaluation of the whole cable with pretension corroded cables.

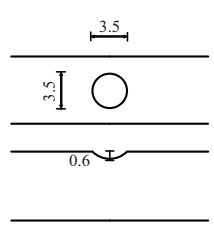
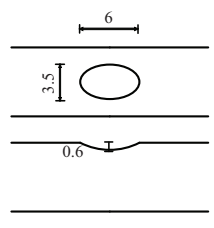
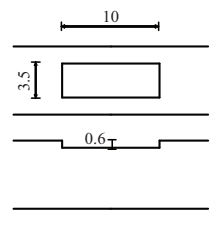
2. Mechanical properties test of high strength steel wire with artificial notch under Tension and bending

2.1. Steel wire sample

The high-strength steel wire used in the test is 1.45 m long and 7 mm in diameter, which is taken from the suspender of a arch bridge cable replacement project. According to the literature investigation, the corrosion pits of steel wire are mainly spherical, ellipsoidal and

grooved [17]. Combined with the statistical data of length, width and depth of corrosion pits of severely corroded steel wire by Okamoto [18], three types of artificial notch is used to simulate the severe corrosion pits of high strength steel wire. Four high strength steel wires are selected for each type of artificial notch. The shape and size of artificial notch of steel wire are shown in Table 1.

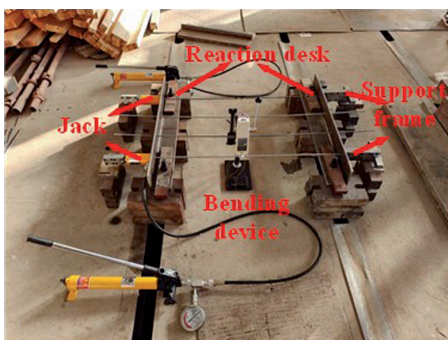
Table 1. Shape and size of artificial notch on steel wire

Notch shape	Dimension /mm	Photograph
Sphere		
Ellipsoid		
Groove shape		

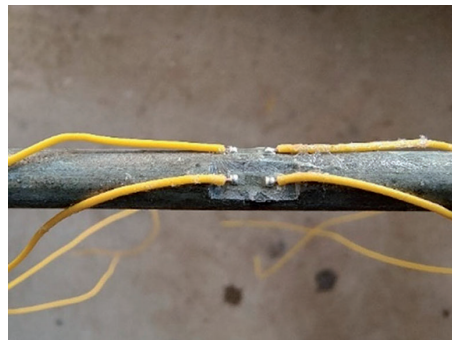
2.2. Test equipment and methods

The test device consists of counter-force frame, Eideburgh digital spring pressure testing machine and a penetrating jack with an oil gauge. During the test, after the pier head treatment of high strength steel wire at both ends, the special fixture is used to anchor the steel wire with artificial notch at one end to the support frame, and the other end is installed with the piercing jack for axial loading. The maximum range of the piercing jack is 50 kN. The pretension of the steel wire is controlled by arranging strain gauges in the intact steel wire section and readings of the jack oil gauge. The bending loading

device adopts Eideburgh digital spring pressure testing machine. The press is equipped with a pressure digital display screen and a displacement distance scale. The range of the pressure digital display screen is 0.0–1000.0 N, and the range of the displacement scale is 0.00–70.00 mm. The applied vertical force and the vertical displacement at the steel wire notch can be read during the bending test loading process. During the test, the steel wire was first passed through the reserved holes along the counterforce frame, and then the support frame was installed close to the pier head. Before the pretension is formally loaded, a small tension is applied to make the support frame fully contact with the pier head so that it does not slide when the pretension is applied. Under different loading directions and different pretension loading conditions, graded bending loading was carried out at the position of the artificial notch on the steel wire. According to the safety factor of the suspender is 3.0 and the yield strength of the test steel wire is 1770 MPa, the allowable stress at the notch is 590 MPa [19]. The vertical displacement of the steel wire is measured by the displacement distance ruler of the pressure testing machine, and the strain gauge is pasted at the bottom of the artificial notch. The strain change at the bottom of the notch during the bending process of the steel wire with notch is measured. The tensile and bending test device and the strain gauge arrangement of the steel wire with notch are shown in Fig. 1.



(a) Tension and bending test device for notched steel wire



(b) Adhesive schematic diagram of notch strain gauge

Fig. 1. Drawing-bending coupling test device and strain gauge layout of steel wire

3. Finite element numerical simulation of notched steel wire under tension and bending

3.1. Material physical parameters and element type

The finite element model of notched strength wire was established by ANSYS WORKBENCH. The steel wire is 7mm in diameter. The total length of the steel wire is 1.45

m. The steel wire material parameters are shown in Table 2. Solid185 and solid186 element are commonly used in steel wire element. The 186 solid unit is a 20-node solid unit, while the 185 solid unit is an 8-node solid unit. The higher order 186 cells are more accurate for entities with larger grid size. In order to select a reasonable element to build a finite element model, two kinds of elements are used to model high strength steel wire with ellipsoidal notch without pretension. According to the calculation, it takes 16 hours and 11 minutes to use solid186 solid element for finite element model calculation. The maximum stress at the notch is 578.9 MPa, and the peak CPU occupancy is 78%, and the running memory occupancy is 99%. However, it only takes 1 hour and 12 minutes to calculate the model with solid185 solid element, and the maximum stress at the notch is 569.7 MPa. Compared with solid186 solid element, the calculation accuracy is 1.59% lower. As can be seen from the above examples, although solid186 element has certain advantages in the accuracy of irregular solid grid division, fine grid division should be carried out at the notch and the model length is long, which leads to the long operation time of solid186 element and the solid185 element can meet the required accuracy requirements. Therefore, solid185 solid element is selected for simulation calculation in this paper.

Table 2. Main parameters of materials

Element type	Wire diameter (mm)	Model length (m)	Elastic modulus (MPa)	Poisson's ratio	Density (kg/m ³)	Yield strength
solid185	7	1.45	2×10^5	0.3	7850	1770

3.2. Load and boundary conditions

According to the test situation, the tensions of 0.25 kN, 0.5 kN and 1 kN were applied at both ends of the model, and the pretension applied by the jack to the high-strength steel wire in the simulation test. Because the loading surface of the pressure testing machine is tangent to the high strength steel wire and the length is 3.5 cm, the bending load is simulated by applying the same line pressure as the tangent length at the model notch, and the bending load is always perpendicular to the steel wire by rotating the coordinate axis. The reaction platforms on both sides are 20 cm away from the steel wire pier head. In the tensile-bending test, the mechanical model of the simply supported beam is adopted. The boundary conditions are set at 20 cm away from both ends of the model, and the degrees of freedom in the *X*-axis and *Z*-axis directions are constrained. In order to apply the pretension, the degrees of freedom in the *Y*-axis direction are released, where the *X*-axis direction is the bending loading direction, and the *Y*-axis direction is the tensile loading direction. The finite element model and the loading situation are shown in Fig. 2. At the same time, opening the software large deformation switch can fully show the influence of pretension on the stiffness of steel wire.

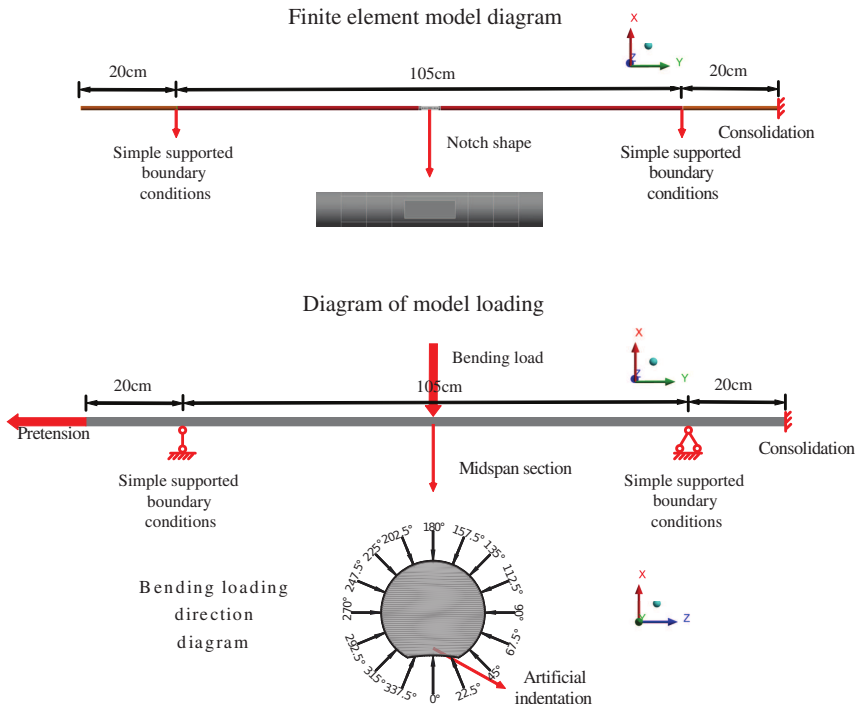


Fig. 2. Finite element model of high strength steel wire with artificial notch (unit: cm)

3.3. Mesh subdivision

In the process of finite element modeling, meshing is very important to the calculation time and result accuracy, and the reasonable mesh density should be selected by considering the calculation scale and calculation accuracy comprehensively. When dividing the mesh, the model is cut first in order to control the mesh density at each position. As the stress change at the notch is mainly studied, 0.09–0.20 mm grid is used in the range of 1.5 cm, 0.20–0.30 mm grid is used in the range of 1.5–3.5 cm, and 1mm grid is used in the rest parts to meet the requirements. The grid division of the three notch is shown in Fig. 3. The total number of elements of spherical notch, ellipsoidal notch and groove notch high strength steel wire finite element models was 1,423,566, 1,700,427 and 1,579,589, respectively.

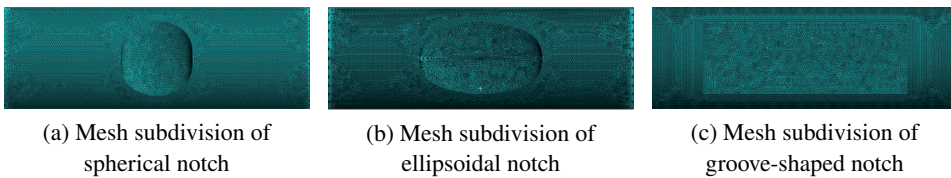
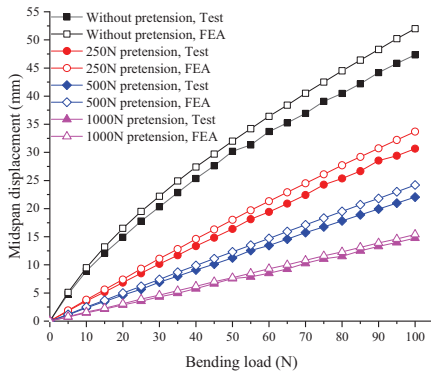


Fig. 3. Drawing-bending coupling test device and strain gauge layout of steel wire

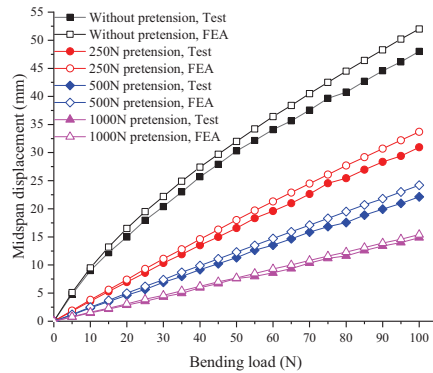
4. Results comparison and analysis

4.1. Effect of Tension on Bending of High Strength Steel Wire with Artificial Notch

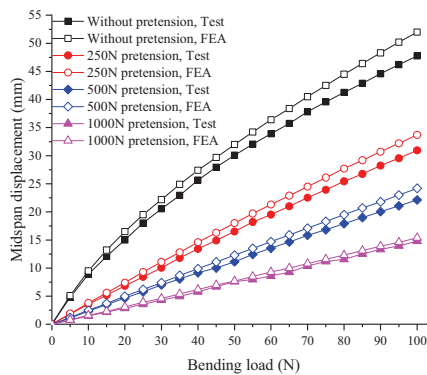
Through the bending tests of three kinds of artificially notched high-strength steel wires, the bending load displacement curve of steel wire midspan is obtained. The test data are compared with the finite element calculation results, and the bending load displacement comparison curve of three kinds of artificially notched steel wires is obtained, as shown in Fig. 4 (Solid point represents test data, hollow point represents finite element analysis data, and FEA represents finite element).



(a) Bending load – displacement curve of spherical steel wire with artificial notch



(b) Bending load – displacement curve of ellipsoidal steel wire with artificial notch



(c) Bending load – displacement curve of grooved steel wire with artificial notch

Fig. 4. Bending load-displacement curves of three kinds of high strength steel wires with artificial notch

It can be seen from Fig. 4 that the experimental data of the bending load-displacement curves of the three kinds of steel wires with artificial notch are basically consistent with the variation law of the finite element numerical simulation results, and show nonlinear changes. In the case of no pretension, the curve shows a line graph with gradually decreasing slope. In the case of pretension, the curve is approximately linear, and with the increase of pretension, the linearity is higher. It can be seen from the curve that the pretension increases the stiffness of high strength steel wire significantly. At the same time, with the increase of pretension, the displacement decreases significantly under the same bending load, and the decrease is the largest when the pretension is initially applied. Under the same bending load, the experimental displacement of high-strength steel wire with artificial notch is slightly smaller than the finite element analysis results. The variation trend of bending load-displacement curve is the same, and the average error of calculated displacement is 7.80 %, which verifies the correctness of the finite element model.

4.2. The influence of loading direction of bending load on the stress at artificial notch

Because the bending load direction of the cable is random in practice, the increase effect of the most unfavorable loading direction on the stress at the artificial notch is studied, and the finite element model of the steel wire is established to analyze the stress variation at the notch. Due to the symmetry of the artificial notch section, combined with the operability and accuracy of the measurement, the stress data loaded in the direction of 90° – 180° are analyzed. Through the calculation of the finite element model, the stress cloud diagram of the three kinds of notch steel wire at the loading moment in the direction of 180° without pretension is shown in Fig. 5.

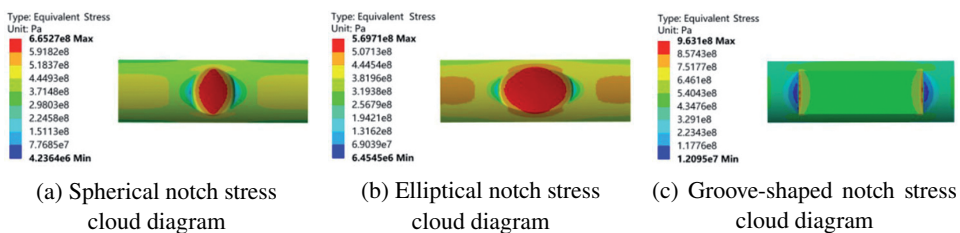
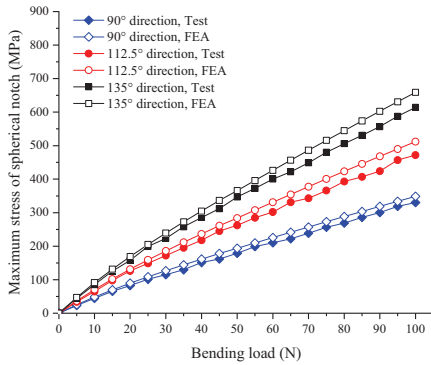
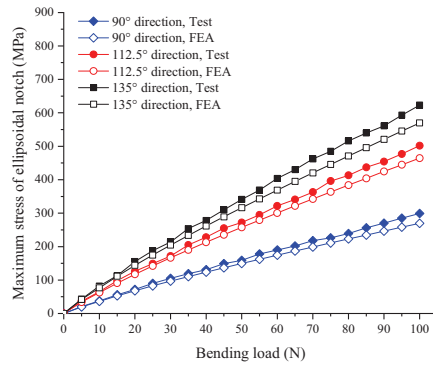


Fig. 5. Finite element stress cloud diagram of three artificial notch loaded in 180° direction without pretension (unit: Pa)

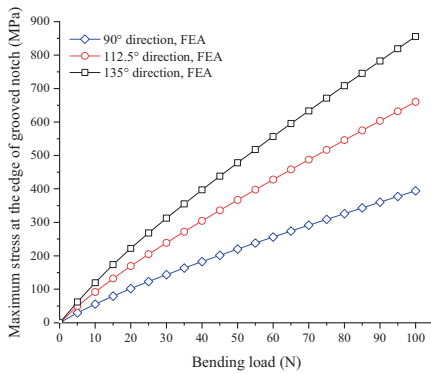
It can be seen from Fig. 5 that under 180° bending loading without pretension, the maximum stresses of spherical and ellipsoidal notch are located at the center of the notch, and the maximum stresses are 665.3 MPa and 569.7 MPa, respectively. The maximum stress of groove-shaped notch occurs at the boundary of the notch, and the maximum values are 963.1 MPa, respectively. The stress changes at the center of groove-shaped notch are relatively uniform. The stress-bending load curves at the bottom of high strength steel wire notch under different bending load directions are shown in Fig. 6.



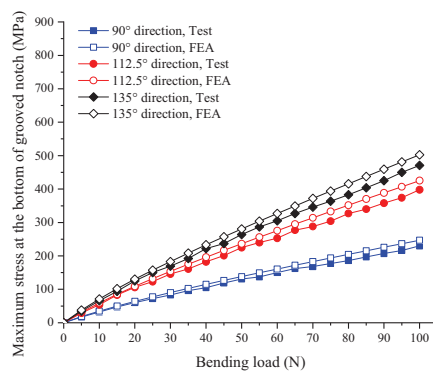
(a) Maximum stress of spherical notch



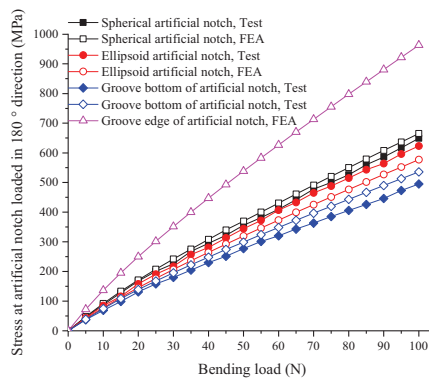
(b) Maximum stress of ellipsoidal notch



(c) Maximum stress of grooved notch



(d) Maximum stress at the bottom of grooved notch



(e) The maximum stress is loaded in 180° direction

Fig. 6. Stress-bending load curve and comparison of different loading directions at artificial notch

It can be seen from Fig. 6 that under different loading directions of bending load, the stress at the bottom of the three kinds of artificial notch and the bending load curve show a nonlinear change trend, and with the decrease of loading angle, the stress at the bottom of the artificial notch also decreases, and the change rule of the test data is consistent with that of the finite element calculation results. When loading at 180° , the bending stress is the largest, and when loading at 90° , the bending stress is the smallest. When the loading direction changed from 180° to 135° under 100 N bending load (corresponding to 48 mm bending displacement), the maximum stress at the edge of spherical, ellipsoidal, grooved and bottom of grooved notch decreased from 665 MPa, 577 MPa, 963 MPa and 536 MPa to 659 MPa, 569 MPa, 855 MPa and 502 MPa, which changed by 0.90%, 1.39%, 11.21% and 6.34%, respectively. The stress at the bottom of spherical and ellipsoidal notch changed little. The maximum stress changes at the edge of grooved notch and at the bottom of grooved notch are obvious; when the loading direction changes from 135° to 90° , the maximum stress at the bottom of spherical, ellipsoidal, grooved and grooved notch decreases from 659 MPa, 569 MPa, 855 MPa and 502 MPa to 348 MPa, 269 MPa, 394 MPa and 247 MPa, respectively, changing by 47.19%, 52.72%, 53.92% and 50.80%. The stress changes at the bottom of the three kinds of notch are obvious, and the stress changes at the bottom of the notch are in the order of spherical, ellipsoidal and grooved notch. However, there is a high stress area at the groove-shaped notch boundary. The comparison and analysis of the test data and the finite element calculation results show that the test stress values at the spherical notch and the grooved notch are slightly smaller than those of the finite element analysis. The curve trends of the test and the model results are the same, and the average errors of the two artificial notch are 7.46% and 7.56%, respectively. However, the experimental stress value of ellipsoidal notch is slightly larger than that of the finite element analysis. However, considering that there is a certain manufacturing error in the processing of the notch steel wire, and the curve trend of the experimental and model results is the same, and the average error is 6.94% by calculation, it is considered that the finite element models of three kinds of artificial notch high strength steel wire are reasonable. In the most unfavorable direction of 180° loading, when the displacement load is 47 mm, 53 mm, 35 mm, spherical notch, ellipsoid notch and groove notch, the maximum stress reaches the safe allowable value of 590 MPa.

4.3. The stress at artificial notch of steel wire under tension and bending

When the angle between the loading direction of bending load and the artificial notch is 180° , the stress at the artificial notch is the largest, which is the most unfavorable stress condition. Therefore, the influence of pretension on the stress of artificial notch is studied, as shown in Fig. 7.

It can be seen from Fig. 7 that the stress-bending load curve at the bottom of the three artificial in is approximately linear under different pretension conditions, and the stress at the notch is basically linear with the increase of pretension. After the pretension is applied, the initial stress will be generated at the artificial notch. With the increase of pretension,

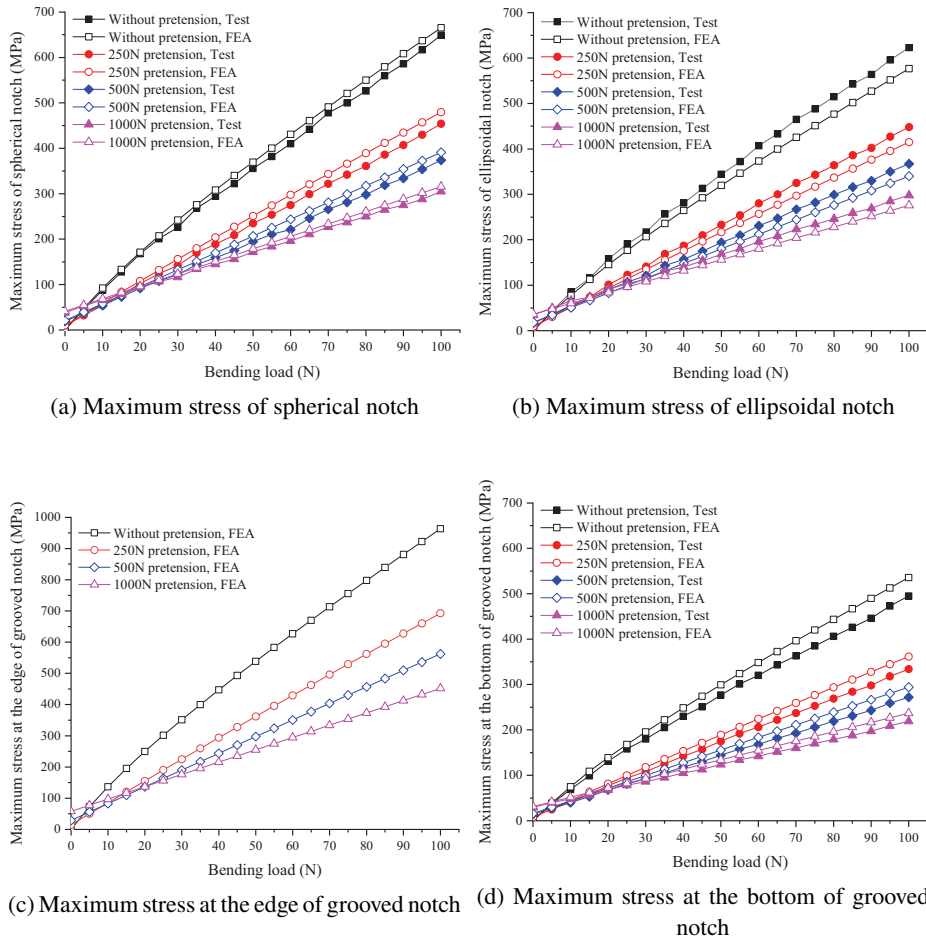


Fig. 7. Stress – bending load curves at loading artificial notch under different pretension and comparison

the initial stress will also increase. However, with the increase of pretension, the bending stiffness of high strength steel wire increases, and the stress produced by bending load at the three artificial notch decreases. When there is no bending load, the greater the pretension, the greater the initial stress at the notch of the steel wire. With the application of bending load and the increase of load value, the bending stress at the notch of high pretension steel wire decreases. In the early stage of pretension, the effect of bending load is the most obvious, with the increase of pretension, the influence degree decreases gradually. Three kinds of artificially notched steel wires under different tension and bending loads, the stress at the spherical notch is the largest, the stress at the ellipsoidal notch is the second, and the stress at the groove notch is the smallest.

5. Conclusion

In this paper, tension and bending tests are carried out on three kinds of artificially notched high-strength steel wires. The refined finite element model of the bending of the notched high-strength steel wire is established by using ANSYS Workbench, and the correctness is verified by the test data. The mechanical properties of the notched steel wire under tension and bending are studied. The main conclusions are as follows:

1. Pretension can improve the stiffness of high strength steel wire and reduce the displacement caused by bending. Under the action of no pretension, the bending load-displacement curve of high strength steel wire is nonlinear. Under the action of pretension, the bending load-displacement curve of high strength steel wire is basically linear, and the linear trend is more obvious with the increase of pretension.
2. Under the action of tension and bending, the stress generated at the bottom of the spherical notch is the largest, followed by the ellipsoidal notch, and the grooved notch is the smallest. However, there is a high stress area at the boundary of the grooved notch, and In the most unfavorable direction of 180° loading, when the displacement load is 47 mm, 53 mm and 35 mm, the maximum stress at the spherical notch ellipsoid notch and groove notch reaches the allowable stress value. In engineering practice, attention should be paid to the mechanical properties of corroded cable section under tension and bending.
3. When vertical loading in the 180° direction, the stress generated at the artificial notch is the largest, and the stress generated by vertical loading in the 90° direction is the smallest. When the vertical loading was changed from 180° to 135°, the maximum stress variation at the bottom of the artificial notch was small, and the maximum stress variation at the bottom of the groove-shaped notch was the largest, with a variation of 6.34%. When the loading was changed from 135° to 90°, the maximum stress variation at the bottom of the artificial notch was very obvious, and the maximum stress variation at the bottom of the ellipsoidal notch was the largest, with a variation of 52.72%.

No matter what kind of notch, it will lead to local stress concentration of the steel wire under the action of tension and bending, and the steel wire in the cable will be in high stress state for a long time. Under the action of repeated bending and shearing, it will lead to fatigue fracture of the steel wire. Through the combination of mechanical test and numerical simulation, this paper studies the mechanical behavior of notched steel wire under tension and bending, which provides a basis for further study of the mechanical properties of corroded cable under tension and bending. The next step is to carry out the experimental and numerical study of cable corrosion distribution and mechanical properties under tension and bending, so as to provide a basis for the evaluation of cable bearing capacity.

Acknowledgements

This paper is supported by the Fundamental Research Funds for the Central Universities(grant number: 2572020BJ02).

References

- [1] Y.L. Chen, H.C. Xu, Y.G. Yu, “Accident analysis of lowered/half supported tied arch bridges and enlightenments for bridge detection”, *Journal of Fujian University of Technology*, 2013, vol. 11, no. 3, pp. 213–217; DOI: [10.3969/j.issn.1672-4348.2013.03.003](https://doi.org/10.3969/j.issn.1672-4348.2013.03.003).
- [2] H.P. Zhao, Y.B. Li, “Study on Damage Degenerating Mechanism and Life Evaluation of Arched Bridge Suspender”, *Urban Roads Bridges & Flood Control*, 2010, no. 1, pp. 119–124.
- [3] J.X. Yang, W.Z. Chen, R. GU, “Analysis of Dynamic Characteristics of Short Hangers of Arch Bridge”, *Bridge Construction*, 2014, vol. 44, no. 3, pp. 13–17.
- [4] A.R. Chen, Y.Y. Yang, R.J. Ma, et al, “Experimental study of corrosion effects on high-strength steel wires considering strain influence”, *Construction and Building Materials*, 2020, vol. 240, pp. 1–12; DOI: [10.1016/j.conbuildmat.2019.117910](https://doi.org/10.1016/j.conbuildmat.2019.117910).
- [5] M. Raoof, T.J. Davies, “Determination of the bending stiffness for a spiral strand”, *Journal of Strain Analysis for Engineering Design*, 2004, vol. 3, no. 1, pp. 1–13.
- [6] K.O. Papailiou, “Bending of helically twisted cables under variable bending stiffness due to internal friction, tensile force and cable curvature”, Ph.D. thesis, University of Stuttgart, Germany, 1995.
- [7] K.J. Hong, C.K. Yi, Y.K. Lee, “Geometry and friction of helically wrapped wires in a cable subjected to tension and bending”, *International Journal of Steel Structures*, 2012, vol. 12, no. 2, pp. 233–242; DOI: [10.1007/s13296-012-2007-9](https://doi.org/10.1007/s13296-012-2007-9).
- [8] S.W. Khan, “Structural characteristics of various types of helically wound cables in bending”, Ph.D. thesis, Loughborough University, 2013.
- [9] F. Foti, L. Martinelli, “A corotational beam element to model the hysteretic bending behavior of metallic wire ropes”, presented at The 4th Canadian Conference on Nonlinear Solid Mechanics, 2013.
- [10] F. Foti, L. Martinelli, “An analytical approach to model the hysteretic bending behavior of spiral strands”, *Applied Mathematical Modelling*, 2016, vol. 40, no. 13-14, pp. 1–13; DOI: [10.1016/j.apm.2016.01.063](https://doi.org/10.1016/j.apm.2016.01.063).
- [11] P. Matuszkiewicz, R. Pigoń, “Parametric analysis of mast guys within the elastic and inelastic range”, *Archives of Civil Engineering*, 2022, vol. 68, no. 1, pp. 169–187; DOI: [10.24425/ace.2022.140162](https://doi.org/10.24425/ace.2022.140162).
- [12] Z.H. Chen, Y.J. Yu, X.D. Wang, et al., “Experimental research on bending performance of structural cable”, *Construction and Building Materials*, 2015, vol. 96, no. 15, pp. 279–288; DOI: [10.1016/j.conbuildmat.2015.08.026](https://doi.org/10.1016/j.conbuildmat.2015.08.026).
- [13] Y.J. Yu, X.X. Wang, Z.H. Chen, “A simplified finite element model for structural cable bending mechanism”, *International Journal of Mechanical Sciences*, 2016, vol. 113, pp. 196–210; DOI: [10.1016/j.ijmecsci.2016.05.004](https://doi.org/10.1016/j.ijmecsci.2016.05.004).
- [14] Y.P. Zhang, Q. Feng, G.N. Wang, et al., “Analytical model for the bending of parallel wire cables considering interactions among wires”, *International Journal of Mechanical Sciences*, 2021, vol. 194, no. 3; DOI: [10.1016/j.ijmecsci.2020.106192](https://doi.org/10.1016/j.ijmecsci.2020.106192).
- [15] Y.P. Zhang, J.F. Wang, G.R. Ye, et al., “Bending Stiffness of Parallel Wire Cables Including Interfacial Slips among Wires”, *Journal of Structural Engineering*, 2018, vol. 144, no. 10; DOI: [10.1061/\(ASCE\)ST.1943-541X.0002171](https://doi.org/10.1061/(ASCE)ST.1943-541X.0002171).
- [16] J.A. Lou, F.Y. Sun, W. Peng, et al., “Study on the effect of uneven corrosion on the stress concentration of high strength steel wire”, *Building Science*, 2018, vol. 34, no. 7, pp. 108–113.
- [17] H.S. Xu, Y.S. Hu, D.H. Yan, “Distribution characteristics of corrosion pit morphology parameters of existing corrosion cable”, *Journal of China and Foreign Highway*, 2020, vol. 40, no. 1, pp. 80–84.
- [18] Y. Okamoto, S. Nakamura, K. Suzumura, “Measurement of corrosion roughness of galvanized bridge wires and fatigue strength of wires with artificial pits”, *Doboku Gakkai Ronbunshuu A*, 2010, vol. 66, no. 4, pp. 691–699; DOI: [10.2208/jsej.66.691](https://doi.org/10.2208/jsej.66.691).
- [19] Y.J. Liu, G.J. Zhang, X.H. Zhou, “Discussion on the value of safety factor of bridge structure”, *China Journal of Highway and Transport*, 2021.